The actin cross-linker Filamin/Cheerio mediates tumor malignancy downstream of JNK signaling

Eva Külshammer and Mirka Uhlirova*

Institute for Genetics and Cologne Excellence Cluster on Cellular Stress Responses in Aging-Associated Diseases (CECAD), University of Cologne, 50674 Cologne, Germany

*Author for correspondence (Mirka.Uhlirova@uni-koeln.de).

Accepted 21 November 2012
Journal of Cell Science 126, 927–938

doi: 10.1242/jcs.114462

Summary

Cell shape dynamics, motility, and cell proliferation all depend on the actin cytoskeleton. Malignant cancer cells hijack the actin network to grow and migrate to secondary sites. Understanding the function of actin regulators is therefore of major interest. In the present study, we identify the actin cross-linking protein Filamin/Cheerio (Cher) as a mediator of malignancy in genetically defined *Drosophila* tumors. We show that in invasive tumors, resulting from cooperation of activated Ras with disrupted epithelial cell polarity, Cher is upregulated in a Jun N-terminal kinase (JNK)-dependent manner. Although dispensable in normal epithelium, Cher becomes required in the tumor cells for their growth and invasiveness. When deprived of Cher, these tumor clones lose their full potential to proliferate and breach tissue boundaries. Instead, the Cher-deficient clones remain confined within the limits of their source epithelium, permitting survival of the host animal. Through interaction with the myosin II heavy chain subunit, Cher is likely to strengthen the cortical actomyosin network and reinforce mechanical tension within the invasive tumors. Accordingly, Cher is required for aberrant expression of genes downstream of the Hippo/Yorkie signaling in the tumor tissue. Our study identifies Cher as a new target of JNK signaling that links cytoskeleton dynamics to tumor progression.

Key words: Tumor invasiveness, Actin dynamics, Myosin II, *Drosophila*, Filamin, Yorkie

Introduction

Establishment of a malignant cell population within formerly healthy tissue involves reprogramming of intracellular signaling circuits as well as alterations of surrounding tissue, permitting cancer cells to survive, proliferate and disseminate (Friedl and Alexander, 2011; Hanahan and Weinberg, 2011). Cell growth and division, cell shape maintenance and cell motility all rely on actin cytoskeleton remodeling in normal as well as in cancer cells (Nürnberg et al., 2011; Pollard and Cooper, 2009; Richardson, 2011). Actin dynamics depends on a plethora of signaling pathways and actin-binding proteins that mediate actin filament growth, bundling, cross-linking and disassembly. Rho GTPases (Rho, Rac, Cdc42) are well known to direct actin filament growth by regulating actin nucleators, the actin related protein-2/3 (Arp2/3) complex and formins (diaphanous-related formins and formin-like proteins), through WAVE/Scar and WASP proteins (Nürnberg et al., 2011) (Fig. 1A). Rho GTPases, cytokines, growth factors or environmental stress can influence actin dynamics through the Jun N-terminal kinase (JNK) pathway (Brumby et al., 2011; Coso et al., 1995; Marinissen et al., 2004; Minden et al., 1995), which modulates expression of specific actin regulatory genes and phosphorylates cytoskeletal components (Xia and Karin, 2004). Aberrant JNK activity has been associated with various tumor types (Wagner and Nebreda, 2009). However, due to the extreme complexity of mammalian tumors, a direct link between JNK, actin, and actual tumor phenotypes has been missing.

The epithelial tumor model that has been established in the fruit fly *Drosophila* (Brumby and Richardson, 2003; Pagliarini and Xu, 2003) offers a relevant yet genetically tractable system where to investigate the contribution of actin dynamics to tumor malignancy. In clones of a columnar epithelium (CE) and a squamous peripodial epithelium (PE) of eye/antennal imaginal disc (EAD), overexpression of an activated form of Ras (Ras^{V12}) induces malignant tumors when combined with disruption of the apico-basal polarity, caused by mutation in one of the tumor suppressors such as Scribble (Scrib), Discs large (Dlg) or Lethal giant larvae (Lgl) (Brumby and Richardson, 2003; Pagliarini and Xu, 2003). These lesions recapitulate hallmarks of mammalian tumors, as the mutant cells overproliferate, resist apoptosis, induce immune response and invade surrounding tissue, ultimately killing the fly larva (Brumby and Richardson, 2003; Cordero et al., 2010; Pagliarini and Xu, 2003; Pastor-Pareja et al., 2008). In this model, activation of JNK together with aberrant Hippo signaling contributes to tumor overgrowth (Doggett et al., 2011; Igaki et al., 2006). At the same time, JNK promotes cell migration and invasion, partly by upregulating expression of matrix metalloprotease 1 (MMP1) (Srivastava et al., 2007; Uhlirova and Bohmann, 2006). The invasive $ras^{V12}scrib^{-/-}$ tumor cells display prominent cortical actin filaments (Leong et al., 2009; Uhlirova and Bohmann, 2006). Interestingly, forced activation of Rho GTPases in cells carrying oncogenic Ras causes a phenotype that resembles the invasive behavior of the $ras^{V12}scrib^{-/-}$ clones (Brumby et al., 2011), thus linking the perturbed actin cytoskeleton dynamics with tumor malignancy.

Our present study discovers an important function of the actin cross-linking protein Cheerio (Cher), a *Drosophila* ortholog of mammalian Filamin A (FLNA) (Sokol and Cooley, 1999), in

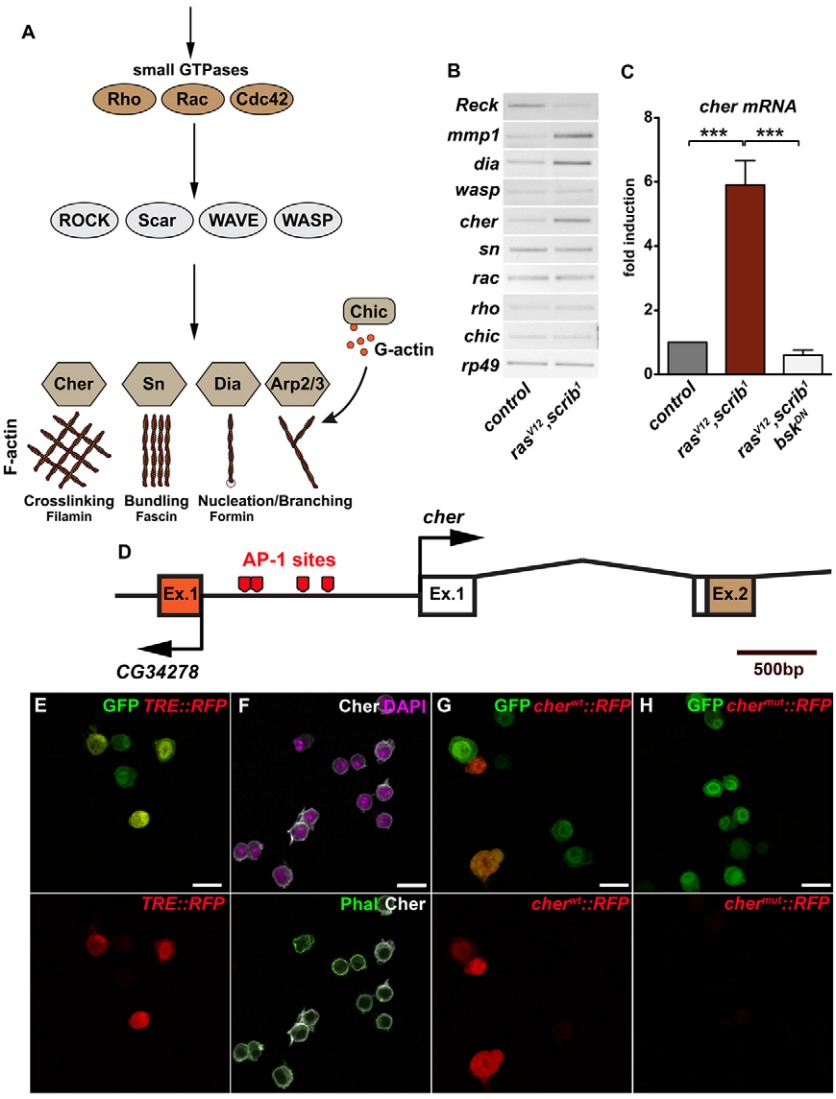

Fig. 1. Upregulation of *cher* in invasive $ras^{V12}scrib^{1}$ tumors requires JNK. (**A**) Proteins regulating actin dynamics. (**B**) *cher*, *dia* and *mmp1* are upregulated whereas *Reck* mRNA declines in EAD bearing malignant $ras^{V12}scrib^{1}$ clones as assessed by semi-quantitative RT-PCR. (**C**) Inhibition of JNK signaling ($ras^{V12}scrib^{1}bsk^{DN}$) results in downregulation of *cher* mRNA as determined by qRT-PCR. Data are means ± s.e.m.; $n=4$; ***$P<0.001$. (B,C) Total RNA was isolated from the mosaic EAD 6 days AEL. Expression of *rp49* is used as a reference. (**D**) Schematic of the 5′ region of the *cher* locus with four putative AP-1 binding sites (T{T,G}A{C,G}TCA). Open and colored boxes represent untranslated and translated exons, respectively. (**E–H**) The AP-1 sites are required for *cher* expression. *Drosophila* S2 cells express a *TRE::RFP* reporter (E), indicating that they possess a functional AP-1 complex. Immunostaining co-localizes endogenous Cher with cortical actin (phalloidin, Phal); nuclei are stained with DAPI (F). The 1.4-kb sequence containing four AP-1 sites ($cher^{wt}$) is sufficient to drive RFP expression (G); mutation of all four AP-1 sites ($cher^{mut}$) abolishes the reporter activity (H). Scale bars: 10 μm.

tumor progression. Filamins are large cytoplasmic proteins whose dimers provide cells with mechanical resilience by cross-linking cortical actin filaments into a dynamic three-dimensional structure. In addition to their role as mechanical linkers, filamins interact with transmembrane receptors, adhesion molecules and even transcription factors, serving as a scaffold during signal transduction (Nakamura et al., 2011; Popowicz et al., 2006). The role of FLNA in tumorigenesis remains controversial. Although downregulation of FLNA expression increases the invasiveness of human breast cancer cells (Cunningham et al., 1992; Xu et al., 2010), a positive effect of FLNA on cell migration has also been reported (Castoria et al., 2011; Cunningham et al., 1992). FLNA expression levels in tumors and plasma of patients with breast and primary brain tumors increase with tumor malignancy (Ai et al., 2011; Alper et al., 2009; Bedolla et al., 2009). Finally, a most recent study has demonstrated that FLNA knockout restrains development of K-Ras induced lung tumors in mice (Nallapalli et al., 2012).

Here, we show that *Drosophila* Filamin/Cher is upregulated in malignant $ras^{V12}scrib^{1}$ tumors in a JNK-dependent manner, and that Cher function is required for tumor growth and invasiveness. In the natural tissue context Cher endows the tumor cells with the lethal capacity to breach the barrier of the PE and invade neighboring organs.

Results

Cher accumulates in invasive clonal tumors

To explore the role the actin filament network plays in tumor malignancy, we searched for actin cytoskeleton-regulating genes that would show altered expression in the eye/antennal imaginal discs (EAD) carrying invasive $ras^{V12}scrib^{1}$ clonal tumors (Brumby and Richardson, 2003; Pagliarini and Xu, 2003). Functions of candidate proteins in actin dynamics are depicted in Fig. 1A. The previously established enrichment of *matrix metalloprotease 1* (*mmp1*) (Uhlirova and Bohmann, 2006) and downregulation of the protease inhibitor *Reck* mRNAs (Srivastava et al., 2007) in $ras^{V12}scrib^{1}$ tumors served for reference (Fig. 1B). We found increased levels of *diaphanous* (*dia*) and *cher* transcripts in $ras^{V12}scrib^{1}$ tumors compared with EAD bearing control clones; expression of the other candidates did not change appreciably (Fig. 1B). A role for diaphanous-like formins in cancer progression is supported by previous studies in

mammalian models (Nürnberg et al., 2011), and effects of *Drosophila* Dia on cell motility (Liu et al., 2010), and regulation of imaginal disc growth (Sansores-Garcia et al., 2011) have been established. We therefore concentrated on the less explored function of the Filamin A (FLNA) ortholog Cher. Using quantitative RT-PCR (qRT-PCR), we confirmed that *cher* mRNA was significantly upregulated in aggressive $ras^{V12}scrib^{1}$ tumors (Fig. 1C). Importantly, *cher* levels correlated with tumor invasiveness as overgrown but noninvasive tumors, in which JNK activity was inhibited by expression of a dominant-negative form of the Jun kinase Basket (Bsk^{DN}), displayed control levels of *cher* mRNA (Fig. 1C).

The EAD consist of a basal CE and an apical PE that face each other with their apical sides (Pallavi and Shashidhara, 2005) and are surrounded by the basal membrane. In addition, circulating blood cells, hemocytes, populate the outer surface of the EAD (Holz et al., 2003). Hemocyte numbers have been shown to increase dramatically in the presence of $ras^{V12}scrib^{1}$ clonal tumors, contributing to their invasiveness (Cordero et al., 2010; Pastor-Pareja et al., 2008). To determine which cell type accumulated Cher, we stained EAD bearing control, $ras^{V12}scrib^{1}$ or $ras^{V12}scrib^{1}bsk^{DN}$ clones with Cher, H2 and Fasciclin III (FasIII) antibodies. Whereas H2 marks hemocytes (Kurucz et al., 2003), FasIII decorates the lateral membranes of both PE and CE epithelia, thus revealing overall EAD morphology.

Control Cher staining was restricted to the apical part of the EAD, marking the PE monolayer (Fig. 2A). Its distribution throughout the EAD was even, with a slight enrichment in the antennal part of the disc. In contrast, Cher expression increased in numerous $ras^{V12}scrib^{1}$ cells located within the PE (Fig. 2B). Disturbed pattern of Cher and FasIII staining indicated that already in early tumors, observed 5 days after egg laying (AEL), the PE morphology became compromised with cells piling atop each other (Fig. 2B″). As clonal tumors continued to grow (7 days AEL) and generate multilayered cell masses, the Cher expression domain expanded basally and the integrity of both the PE and CE deteriorated (supplementary material Fig. S1A). Cher showed a similar pattern of enrichment in invasive $ras^{V12}dlg^{1}$ tumors (supplementary material Fig. S1B).

As expected, few hemocytes attached to control EAD or those carrying noninvasive $ras^{V12}scrib^{1}bsk^{DN}$ tumors (Fig. 2A,C), whereas invasive $ras^{V12}scrib^{1}$ or $ras^{V12}dlg^{1}$ tumors attracted great numbers of hemocytes (Fig. 2B, supplementary material Fig. S1B). However, the hemocytes expressed Cher regardless of the tumor genotype (Fig. 2). Therefore, both the PE and the associated hemocytes contributed to normal Cher expression within the EAD and to its increase upon induction of $ras^{V12}scrib^{1}$ or $ras^{V12}dlg^{1}$ tumor clones. However, although Cher from the hemocytes accumulated due to higher hemocyte population, elevated *cher* expression in the clonal tumors required JNK activity.

JNK-dependent *cher* activation

Inhibition of JNK signaling, achieved either by expressing Bsk^{DN} or removing the transcription factor Fos (encoded by *kayak*), reduced the Cher signal within $ras^{V12}scrib^{1}bsk^{DN}$ (Fig. 2C) and $ras^{V12}scrib^{1}kay^{3}$ (supplementary material Fig. S1C) clones, respectively. The reduction was to levels seen in the surrounding wild-type tissue, suggesting that basal *cher* expression in EAD did not depend on JNK. To test whether *cher* might be activated by JNK signaling directly, we examined four putative AP-1 sites that occur within 1.4 kb upstream of the first untranslated *cher* exon (Fig. 1D). AP-1 motifs are recognized by Activating Protein 1, a dimer of bZIP proteins such as Jun and Fos, acting downstream of JNK (Kockel et al., 2001). Wild-type and mutated versions of the 1.4-kb region were tested for transcriptional activity in *Drosophila* S2 cells that possess a functional AP-1 complex, as evidenced by activation of a TPA-dependent *TRE::RFP* reporter (Fig. 1E) (Chatterjee and Bohmann, 2012). Consistent with the presence of endogenous Cher in S2 cells (Fig. 1F), we observed high activity of the $cher^{wt}$*::mRFP* reporter (Fig. 1G). When all four AP-1 sites were mutated ($cher^{mut}$*::mRFP*) the expression was lost (Fig. 1H), indicating that the AP-1 motifs were essential.

To test whether activation of JNK signaling was sufficient to stimulate *cher* transcription, we overexpressed the JNKK Hemipterous (Hep^{wt}) in third-instar larvae using the conditional TARGET system, which enables heat-inducible ubiquitous expression of UAS-driven transgenes (McGuire et al., 2003). Quantitative RT-PCR showed that expression of the known JNK target gene *puckered* (Martín-Blanco et al., 1998) and of *cher* was induced in response to the temporary JNK activation *in vivo* (supplementary material Fig. S2). Together, the results show that the JNK pathway is necessary and sufficient for activating *cher* transcription above its basal level.

Cher is required for tumor cell proliferation

The strong JNK-dependent upregulation of Cher expression in $ras^{V12}scrib^{1}$ tumors raised the question whether Cher might be required for JNK-mediated tumor growth and invasiveness (Igaki et al., 2006; Uhlirova and Bohmann, 2006; Leong et al., 2009; Brumby et al., 2011). To this end, we utilized a $UAS\text{-}cher^{IR}$ (RNAi) transgenic fly line and a previously described protein-null allele $cher^{1}$ (Robinson et al., 1997; Sokol and Cooley, 1999), and tested their ability to modify tumor phenotypes. Removing Cher using either method in mitotic clones induced within the developing EAD had no impact on clone number or morphology, and resulted in adults with regular eyes (supplementary material Fig. S3A–C). Cher is therefore dispensable for normal eye development.

However, loss of *cher* markedly interfered with the growth of $ras^{V12}scrib^{1}$ tumors. On day 7 AEL, the size of $ras^{V12}scrib^{1}$ clones increased dramatically at the expense of surrounding wild-type tissue in both the eye and antenna parts of the EAD (Fig. 3A). The tumor mass became strongly reduced in Cher-deficient $ras^{V12}scrib^{1}cher^{1}$ clones, mainly within the antenna part (Fig. 3B; supplementary material Fig. S4). FACS sorting of cells from EAD dissected on days 6 and 7 AEL confirmed that the apparent decline in number of GFP-positive cells in $ras^{V12}scrib^{1}cher^{1}$ EAD clones was indeed significant (Fig. 3C).

To discern whether the absence of *cher* function impaired tumor cell viability or proliferation, we quantified cells positively staining with apoptotic (activated caspase 3) and mitotic (phospho-histone 3, pH 3) markers in clonal (GFP^{+}) and surrounding (GFP^{-}) EAD tissue upon FACS sorting (Fig. 3D). Although caspase-3-positive cells occurred in EAD harboring both $ras^{V12}scrib^{1}$ and $ras^{V12}scrib^{1}cher^{1}$ clones, particularly at the clonal boundaries (supplementary material Fig. S4A,B), the loss of Cher caused no change in the incidence of apoptosis in either the clonal or the surrounding EAD cell populations (Fig. 3D). Therefore, Cher deficiency did not compromise tumor cell

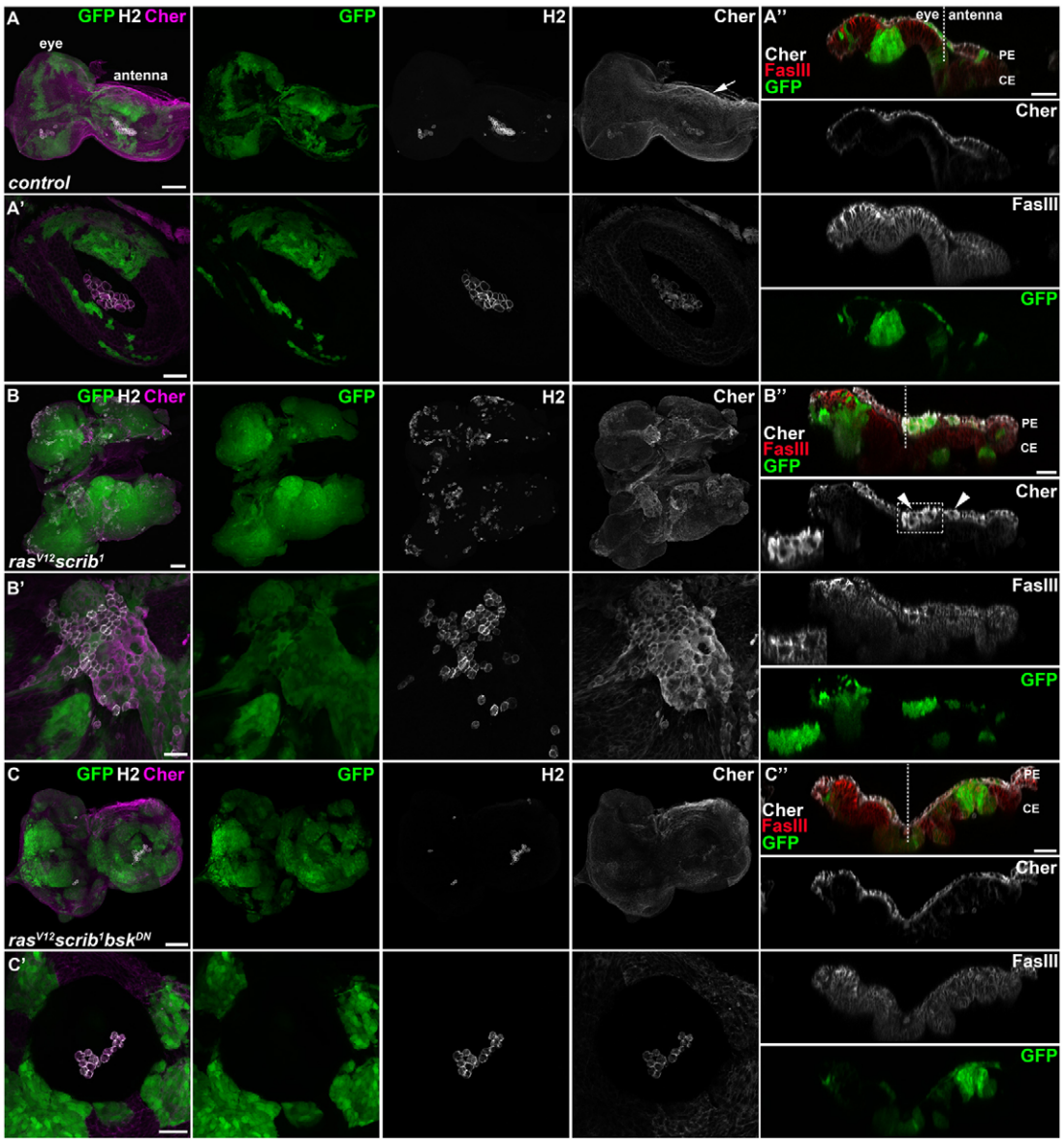

Fig. 2. Cher is enriched within *ras*^{V12}*scrib*^{1} clones. (**A**) In EAD carrying control clones (marked by GFP), Cher occurs in the peripodial epithelium (PE) with enrichment on the medial side of the antenna (arrow; see also supplementary material Fig. S3A), and in EAD-associated hemocytes (A′). (**B**) In EAD harboring tumors, Cher accumulates in apical *ras*^{V12}*scrib*^{1} clones (B″, arrowheads) and hemocytes (B′). The disorganized pattern of Cher and FasIII staining (B″, dotted rectangle) indicates compromised integrity of the PE. (**C**) In *ras*^{V12}*scrib*^{1}*bsk*^{DN} clones, Cher signal decreases to levels in the surrounding normal tissue while it remains high in the hemocytes. The number of hemocytes decreases relative to *ras*^{V12}*scrib*^{1} EAD. All panels are confocal images of third-instar EAD, aged 6 days (A,C), 7 days (B) and 5 days (A″,B″,C″) AEL. Panels show maximum intensity projections of multiple confocal sections; panels are magnified views of apically localized clones. Images A″, B″ and C″ show single transversal sections of the entire EAD with the apical side up; the dashed lines delimit the eye and antennal parts of the EAD. Posterior is to the left in all panels. Scale bars: 50 μm (A–C), and 20 μm (A′–C′, A″–C″).

viability. Normally developing eye discs show two rows of mitotic cells along the morphogenetic furrow, and asynchronously dividing cells anterior to the furrow (supplementary material Fig. S5A). The presence of overgrowing *ras*^{V12}*scrib*^{1} clones doubled the incidence of pH 3-positive cells predominantly within the clonal (GFP^{+}) tissue (Fig. 3D; supplementary material Fig. S5B), and this increase required Cher (Fig. 3D). Interestingly, EAD carrying *ras*^{V12}*scrib*^{1}*cher*^{1} clones also displayed extra cell divisions which, however, mainly occurred within the non-clonal surrounding tissue (Fig. 3D; supplementary material Fig. S5C). Based on these data we conclude that Cher is cell-autonomously required for proliferation of *ras*^{V12}*scrib*^{1} tumors but not for their survival.

Although the absence of *cher* function limits tumor cell proliferation, it promotes cell differentiation within the EAD clonal tumors. Scarce Elav-positive cells confirmed that most *ras*^{V12}*scrib*^{1} cells failed to differentiate into neurons (Fig. 3A) (Brumby and Richardson, 2003; Uhlirova et al., 2005). Despite sizable *ras*^{V12}*scrib*^{1}*cher*^{1} clones located posterior to the morphogenetic furrow, the number of Elav-positive differentiating photoreceptors increased and their organization

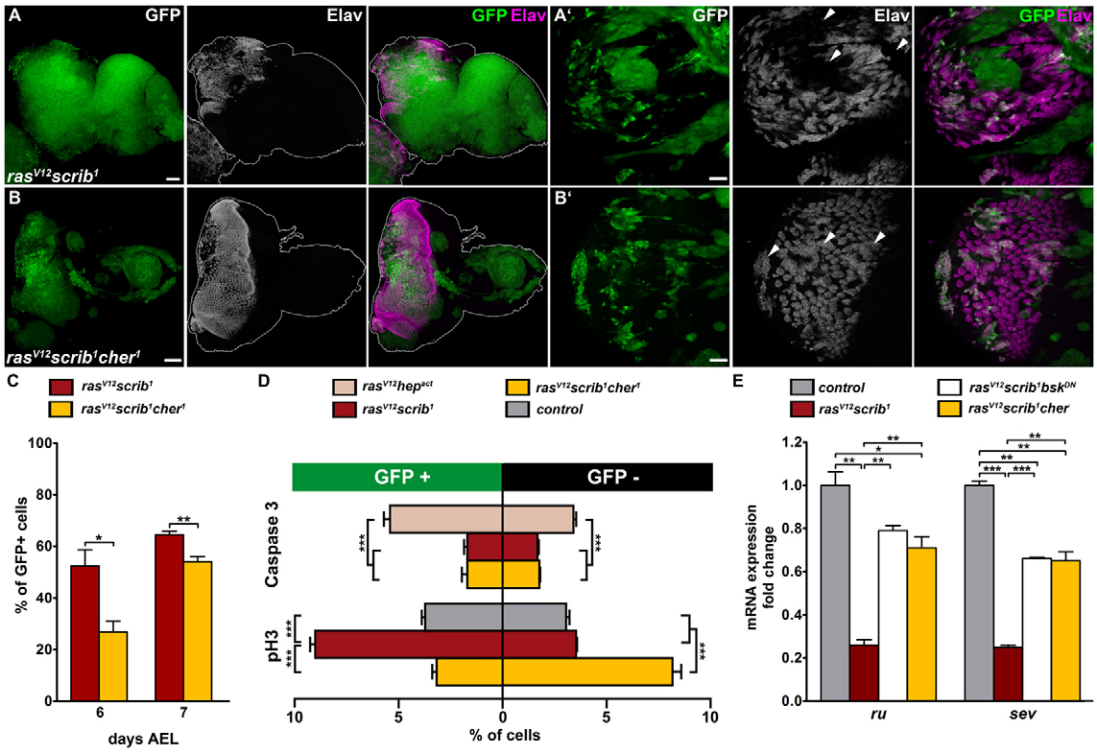

Fig. 3. Cher promotes proliferation of undifferentiated *ras^{V12}scrib^{1}* tumors. (**A**) *ras ^{V12}scrib^{1}* clones (GFP) overgrow the entire EAD and prevent photoreceptor differentiation, marked by Elav. Note the irregular shape and lack of structured ommatidial clusters (A′, arrowheads) within the Elav domain. (**B**) *ras^{V12}scrib^{1}cher^{1}* clones are smaller compared with *ras^{V12}scrib^{1}* clones and many clonal GFP^{+} cells label Elav positive (B′, arrowheads); the typical shape of the EAD is preserved. All images show EAD 7 days AEL, either as projections of multiple confocal sections (A,B) or single sections (A′,B′). White outlines of the EAD were drawn based on staining with DAPI (not shown). Posterior is to the left. Scale bars: 50 µm (A,B), and 20 µm (A′,B′). (**C**) Percentage of GFP^{+} cells within EAD bearing clones of the indicated genotypes was determined by FACS sorting on days 6 and 7 AEL. (**D**) Proportions of apoptotic (active caspase 3) and mitotic (pH 3) clonal (GFP^{+}) and non-clonal (GFP$^{−}$) EAD cells determined by FACS at 6 days AEL. As expected, augmentation of JNK signaling by Hep^{act} increased cell death (Uhlirova et al., 2005). Removal of Cher from *ras^{V12}scrib^{1}* clones did not affect viability but limited clonal cell proliferation while stimulating compensatory growth in surrounding (GFP$^{−}$) tissue. (**E**) Expression of *roughoid* (*ru*) and *sevenless* (*sev*) in EAD (6 days AEL) bearing clones of the indicated genotypes was determined by qRT-PCR. Data in (C–E) are means ± s.e.m.; $n \geq 3$; *$P<0.05$, **$P<0.01$ and ***$P<0.001$.

improved relative to *ras^{V12}scrib^{1}* clones (Fig. 3A,B). Consequently, well-ordered arrays of ommatidia appeared in *ras^{V12}scrib^{1}cher^{1}* EAD compared with the indiscernible pattern in *ras^{V12}scrib^{1}* discs (supplementary material Fig. S5B,C). Further, removal of Cher from *ras^{V12}scrib^{1}* clones improved expression of the *roughoid* and *sevenless* genes that promote photoreceptor specification (Fig. 3E). Expression of both genes was similarly restored in noninvasive *ras^{V12}scrib^{1}bsk^{DN}* clones (Fig. 3E) that displayed reduced *cher* activity (Fig. 1C; Fig. 2C).

Cher deficiency suppresses tumor invasiveness and lethality

A closer examination of EAD uncovered differences in morphology and distribution of *ras^{V12}scrib^{1}* versus *ras^{V12}scrib^{1}cher^{1}* clones. The former were found within both the PE and CE (Fig. 2B″; Fig. 4C; supplementary material Fig. S1A). Many apically localized *ras^{V12}scrib^{1}* cells were elongated and besides strong Cher expression they also showed upregulation of MMP1 and massively enriched cortical actin fibers (Fig. 4A; supplementary material Fig. S6A–C). In contrast, cross-sections of *ras^{V12}scrib^{1}cher^{1}* EAD revealed that large tumors only resided within the basal compartment of the CE (Fig. 4D). Smaller *ras^{V12}scrib^{1}cher^{1}* clones were confined between the PE and CE (Fig. 4D); their round, cyst-like shape was highlighted by cortical actin (Fig. 4B). Finally, only few Cher-deficient clones found within the PE were often surrounded by non-clonal cells extending long, Cher-rich protrusions between and over the clonal cells (Fig. 4E,F). Consequently, the PE appeared largely intact (Fig. 4D). The infrequent *ras^{V12}scrib^{1}cher^{1}* apical clones and those enclosed within the epithelia still expressed MMP1 (supplementary material Fig. S6D–F). *mmp1* mRNA was only slightly lowered in EAD bearing *ras^{V12}scrib^{1}cher^{1}* relative to *ras^{V12}scrib^{1}* tumors (supplementary material Fig. S6G), indicating that Cher was dispensable for JNK-mediated MMP1 expression.

The reduced number of apical clonal tumors and improved PE integrity suggested that removal of Cher might curb tumor spreading, as fewer MMP1-producing cells were in the position to attack the basal membrane. Indeed, we found that in contrast to highly invasive *ras^{V12}scrib^{1}* clonal tumors, fewer *ras^{V12}scrib^{1}cher^{1}* clones invaded the brain and the ventral nerve cord (Fig. 5A,B). Unbiased estimation of tumor grade (see Materials and Methods) showed that invasive behavior of *ras^{V12}scrib^{1}cher^{1}* tumors was significantly reduced ($P \leq 0.001$) compared with *cher^{+}* clones. Suppression of tumor invasiveness

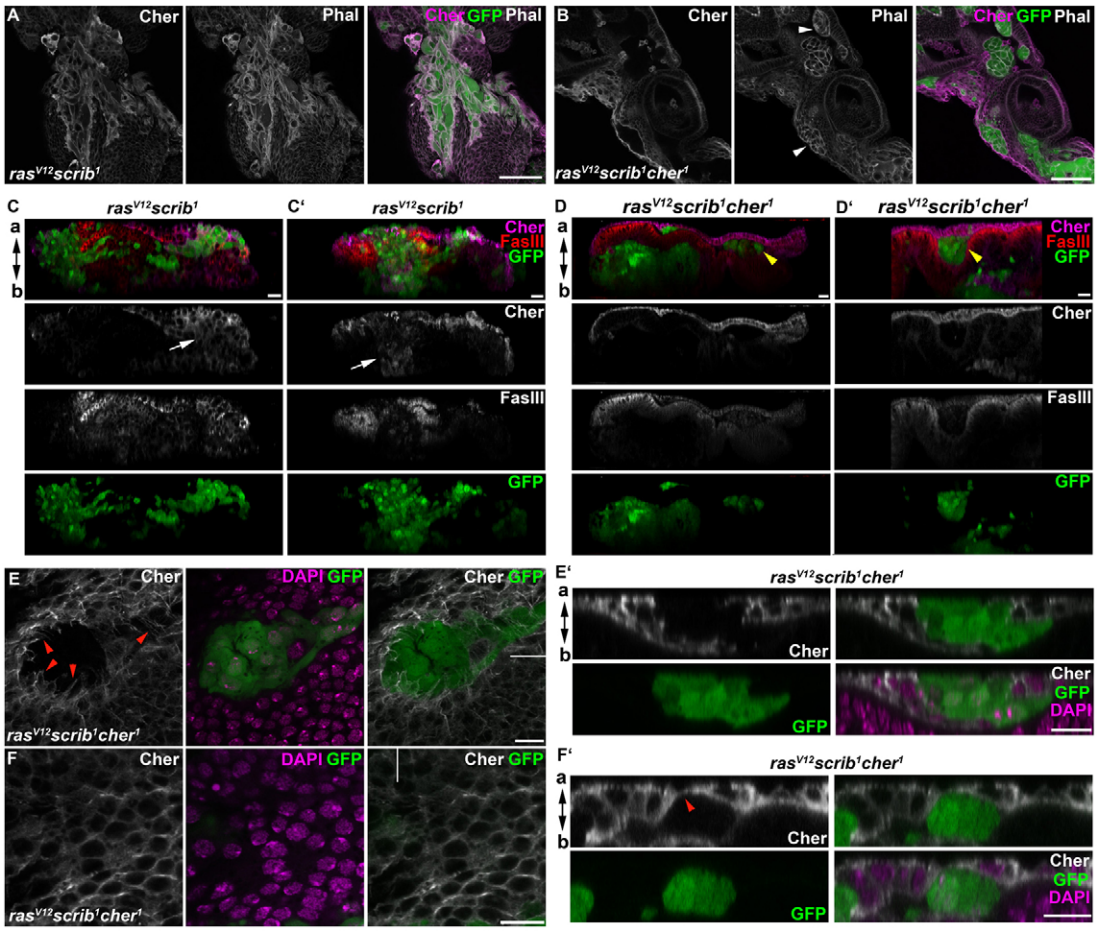

Fig. 4. Cher-deficient tumors are eliminated from the peripodial epithelium and contained within epithelial boundaries. (**A**) Elongated *ras*^{V12}*scrib*^{1} cells within the PE show high Cher levels and prominent actin filaments marked with phalloidin (Phal). (**B**) *ras*^{V12}*scrib*^{1}*cher*^{1} clones retain enhanced cortical actin levels while assuming round, cyst-like morphology (white arrowheads). (**C**) Multilayered *ras*^{V12}*scrib*^{1} tumors occupy both the PE and CE with Cher expression expanding basally (white arrow). FasIII staining reveals disturbed apico-basal (a–b) polarity. (**D**) Large *ras*^{V12}*scrib*^{1}*cher*^{1} clones locate only basally within the CE while small clones are confined between PE and CE. Note the smooth, round edges of *ras*^{V12}*scrib*^{1}*cher*^{1} clones compared with *ras*^{V12}*scrib*^{1} clones. Epithelial integrity is well preserved as shown by continuous Cher and FasIII staining. (**E**,**F**) Apical *ras*^{V12}*scrib*^{1}*cher*^{1} clones are surrounded by non-clonal PE cells emanating Cher-rich protrusions (red arrowheads) towards the clonal cells. White lines mark the position of the respective transversal sections. Images in A, B, E and F are single apical confocal sections; C, D, E′ and F′ are transversal sections of EAD with the apical side up. Scale bars: 50 μm (A,B), 10 μm in all other panels.

was also achieved by Cher depletion in *ras*^{V12}*scrib*^{1} clones using RNAi ($P \leq 0.001$) (Fig. 5C).

Strikingly, elimination of Cher from *ras*^{V12}*scrib*^{1} clones improved animal viability. Larvae bearing *ras*^{V12}*scrib*^{1} tumors all die in the third instar and never pupate (Pagliarini and Xu, 2003; Uhlirova and Bohmann, 2006; Brumby and Richardson, 2003). In contrast, on day 8–9 AEL, 30% of *ras*^{V12}*scrib*^{1}*cher*^{1} larvae began to wander and pupate (Fig. 5D), albeit 2–3 days later than control animals. Thirty percent of *ras*^{V12}*scrib*^{1}*cher*^{1} pupae then emerged as adults. Interestingly, these flies had abnormally enlarged eyes with folded surface, accommodating surplus ommatidia (Fig. 5E–G). Consistent with impaired proliferation of clonal cells in EAD of third-instar larvae, the adult eyes contained only few GFP^{+} cells (Fig. 5F′), suggesting that the superfluous adult tissue most likely originated from extra mitotic activity that was observed outside the mutant clones (Fig. 3D; supplementary material Fig. S5C).

Cher interacts with nonmuscle myosin II to promote tumor malignancy

Processes affected by Cher deficiency in the tumor cells, including changes in cell shape, proliferation and motility, likely involve actomyosin contractions. It has been well established that epithelial tumors exhibit increased cell-generated forces through actomyosin contractility that enhance their growth, survival and invasiveness (Butcher et al., 2009). It is therefore plausible that the increased Cher levels provide *ras*^{V12}*scrib*^{1} tumors with the advantage of extra-resilient actomyosin network. Cher has been previously co-localized with nonmuscle myosin II (MyoII) heavy chain, encoded by the *zipper* (*zip*) locus, to the cleavage furrow of dividing *Drosophila* cells (Field and Alberts, 1995). Our immunostaining of EAD bearing control and *ras*^{V12}*scrib*^{1} clones revealed overlapping patterns of Cher and Zip proteins (Fig. 6A,B). However, *ras*^{V12}*scrib*^{1} tumors showed enrichment of both Cher and Zip relative to the surrounding non-clonal tissue (Fig. 6B).

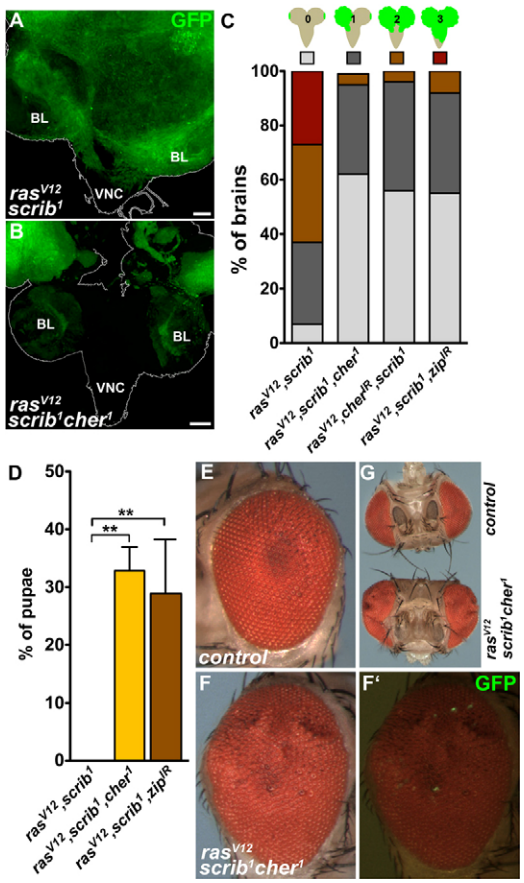

Fig. 5. Cher is required for tumor invasiveness. (**A**,**B**) At 7 days AEL, $ras^{V12}scrib^{1}$ clones (GFP) cover both brain lobes (BL) and spread to the ventral nerve cord (VNC), whereas $ras^{V12}scrib^{1}cher^{1}$ clones are suppressed. Organ outlines were drawn based on DAPI staining (not shown). (**C**) Mutational loss ($ras^{V12}scrib^{1}cher^{1}$) or RNAi depletion of Cher ($ras^{V12}scrib^{1}cher^{IR}$) or Zip ($ras^{V12}scrib^{1}zip^{IR}$) significantly reduces tumor invasiveness (chi-square, $P \leq 0.001$). Four schematically depicted grades of tumor invasiveness were scored based on spreading of clonal GFP^{+} tissue in brains dissected 7 days AEL (see the Materials and Methods section). Results are percentage of brains falling into each category. (**D**) Loss of either Cher or Zip from $ras^{V12}scrib^{1}$ clones improves pupation rate. Data are means ± s.e.m.; $^{**}P<0.01$. (**E–G**) Eyes of adults recovered from larvae carrying $ras^{V12}scrib^{1}cher^{1}$ EAD clones are larger than normal, with extra ommatidia resulting in a wavy surface. Yet only few ommatidia appear GFP positive (F′), suggesting overgrowth of non-clonal tissue. The enlarged eye size affects the entire head (G). Scale bars: 50 μm.

These results prompted us to test whether Cher and Zip form a complex. Indeed, we were able to co-precipitate Cher with Zip in lysates from EAD bearing control clones or $ras^{V12}scrib^{1}$ tumors, the latter showing apparently higher amounts of the individual proteins and of their complex (Fig. 6E). Besides enrichment for Cher and Zip, $ras^{V12}scrib^{1}$ clones also accumulated phosphorylated myosin II regulatory light chain, a product of the *spaghetti squash* gene (*sqh*) (Karess et al., 1991) that marks sites of active actomyosin contraction (Fig. 6C). Strikingly, no such enhancement of p-Sqh relative to the non-clonal tissue was found in $ras^{V12}scrib^{1}cher^{1}$ clones (Fig. 6D), although these clones still contained increased levels of the myosin II heavy chain Zip (supplementary material Fig. S7). Therefore, loss of Cher appears to affect MyoII activity.

To address the importance of the Cher-Zip interaction for malignancy of $ras^{V12}scrib^{1}$ cells, we removed Zip from the tumor clones using an RNAi *UAS-zip*^{IR} transgene. Depletion of Zip coincided with decreased p-Sqh levels whereas Cher and cortical actin remained enriched within $ras^{V12}scrib^{1}zip^{IR}$ clones (Fig. 6F,G). Importantly, reduced occurrence of Zip lessened tumor invasiveness and improved pupation rate to an extent similar to the effect of Cher deficiency (Fig. 5C,D). Taken together, these data indicate that enrichment of the mutually interacting Cher and Zip proteins and enhanced MyoII contractile activity promotes growth and invasiveness of $ras^{V12}scrib^{1}$ tumor clones.

Cher is required for expression of downstream targets of Yorkie

Recent studies in *Drosophila* show that increased mechanical tension promotes tissue overgrowth via inhibition of Hippo (Hpo) signaling (Fernández et al., 2011; Sansores-Garcia et al., 2011). Suppression of Hpo allows the transcriptional co-activator Yorkie (Yki) to turn on genes such as *expanded* (*ex*) and *dally* (Baena-Lopez et al., 2008; Hamaratoglu et al., 2006). Enhanced Yki activity has been previously detected in $ras^{V12}scrib^{1}$ clones (Doggett et al., 2011). Our data indicated that Cher may reinforce mechanical tension within the tumor tissue by interacting with the actomyosin network. We therefore tested whether expression of Yki targets in $ras^{V12}scrib^{1}$ clones might require Cher. Indeed, we found that the activity of an *expanded* reporter (*ex::lacZ*) (Boedigheimer and Laughon, 1993) as well as the levels of *ex* and *dally* mRNAs were clearly lower in EAD carrying Cher-deficient clones relative to those with $ras^{V12}scrib^{1}$ clones (Fig. 7). Immunostaining with an anti-β-Gal antibody showed that upregulated *ex::lacZ* expression colocalized with $ras^{V12}scrib^{1}$ clones and that *cher* deficiency resulted in cell-autonomous reduction of the reporter activity (Fig. 7F,G). Consistent with the previous report (Doggett et al., 2011), inhibition of Hpo signaling in $ras^{V12}scrib^{1}$ mosaic EAD appeared independent of JNK (Fig. 7C,E). Thus, Cher is necessary in $ras^{V12}scrib^{1}$ tumors to suppress the output from the Hpo pathway. These data suggest a possible link between Cher-dependent mechanical tension and attenuation of Hpo signaling in the tumor context.

Discussion

Although actin cytoskeleton has been primarily linked with cell migration of normal as well as cancer cells, roles of the actin network in numerous other processes have emerged. The involvement of the actin cross-linking protein FLNA in cancer development has been suggested but poorly defined, as *FLNA* expression can correlate both positively and negatively with malignant tumor progression (Alper et al., 2009; Xu et al., 2010). Latest data from a mouse model support a tumor-promoting role of FLNA in K-Ras induced lung cancer (Nallapalli et al., 2012). In this study we demonstrate the contribution of the *Drosophila* FLNA ortholog, Cher, to aggressive growth and invasiveness of malignant clonal tumors.

We propose a model for Cher function in tumor malignancy (Fig. 8). In the presence of Cher, $ras^{V12}scrib^{1}$ clones form tumors that rapidly proliferate within both the PE and CE. JNK-dependent upregulation of MMP1 activity in apical (PE) clones and increased mechanical force generated by the quickly expanding tumor mass cooperatively destroy the basement membrane barrier, allowing tumor cells to depart from the disc

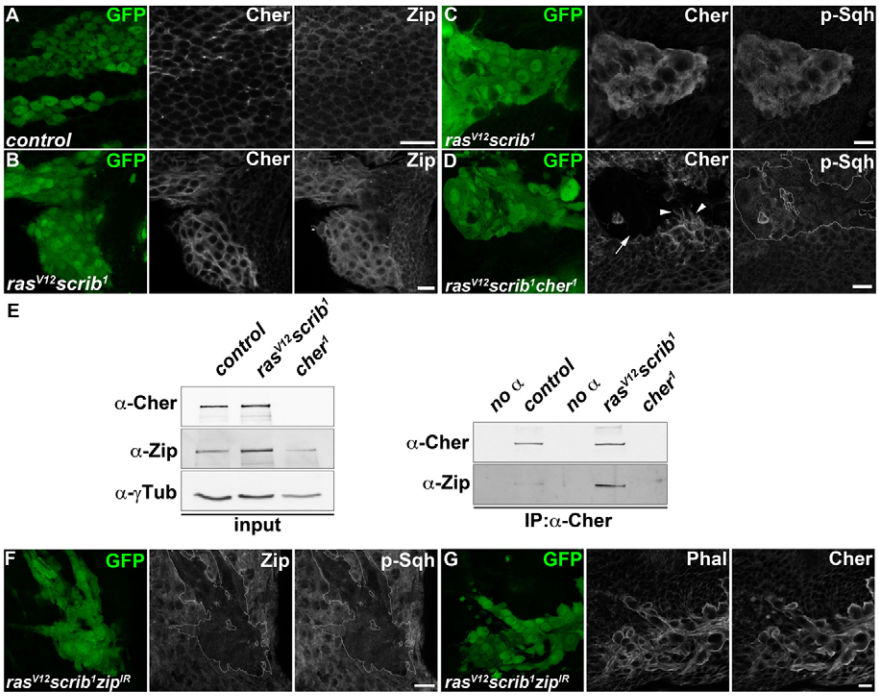

Fig. 6. Interaction between Cher and myosin II. (**A**,**B**) In EAD bearing control (A) and *ras*^{V12}*scrib*^{1} (B) GFP-positive clones, Cher co-localizes with myosin II heavy chain (Zip); both proteins are enriched in *ras*^{V12}*scrib*^{1} clones. (**C**,**D**) Phosphorylated myosin II regulatory light chain (p-Sqh) accumulates in *ras*^{V12}*scrib*^{1} but not in *ras*^{V12}*scrib*^{1}*cher*^{1} clones. (**E**) Immunoblot (left) shows increased levels of Cher and Zip proteins in lysates from *ras*^{V12}*scrib*^{1} mosaic EAD relative to control tissue. Note the absence of Cher in EAD lysate from *cher*^{1} homozygotes. Anti-γ-tubulin served as a control for equal loading. Immunoprecipitation with anti-Cher antibody (right) recovered more Zip from *ras*^{V12}*scrib*^{1} EAD compared with control. Using no primary antibody (no α) and lysate from *cher*^{1} animals confirmed the specificity of the interaction, (**F**,**G**) Depletion of Zip diminished p-Sqh while F-actin and Cher remained high in *ras*^{V12}*scrib*^{1}*zip*^{IR} clones relative to non-clonal tissue. All microscopy images are single confocal sections. Clonal areas are outlined. Scale bars: 10 μm.

and invade surrounding organs. In addition, destruction of the basement membrane and secretion of JAK/STAT activating cytokines induce proliferation of circulating hemocytes (Pastor-Pareja et al., 2008), which further enhance tumor growth and spreading (Cordero et al., 2010). Enrichment in the cortical actin filaments and the Cher complex with MyoII provide the tumor cells with resilience sufficient to withstand increased mechanical stress and with extra contractility to promote their proliferation and invasion. Conversely, removal of Cher from *ras*^{V12}*scrib*^{1} clones slows their proliferation down, particularly within the PE, so that fewer MMP1-producing cells directly face the basement membrane and may attack its integrity. Consequently the reduced tumor mass remains contained within the largely intact PE, which therefore presents a physical barrier to the tumors.

Interestingly, tumors but not normal eye/antennal imaginal epithelia require Cher function. We show that in the EAD of third-instar larvae, Cher protein localizes primarily to the PE, a monolayer of polarized cells that lie between the CE and the basal membrane. Consistent with the absence of an externally visible eye phenotype in *cher* mutant flies (Li et al., 1999; Sokol and Cooley, 1999), loss of Cher from EAD clones had no obvious effect (supplementary material Fig. S3). Cher function, however, becomes needed in the context of rapidly growing and invasive tumors. We found that similar to MMP1 (Srivastava et al., 2007; Uhlirova and Bohmann, 2006), Cher was upregulated in EAD carrying *ras*^{V12}*scrib*^{1} clones in JNK and Fos dependent manner. The enhanced Cher expression originated from tumor cells within the PE, yet with tumors growing into undifferentiated

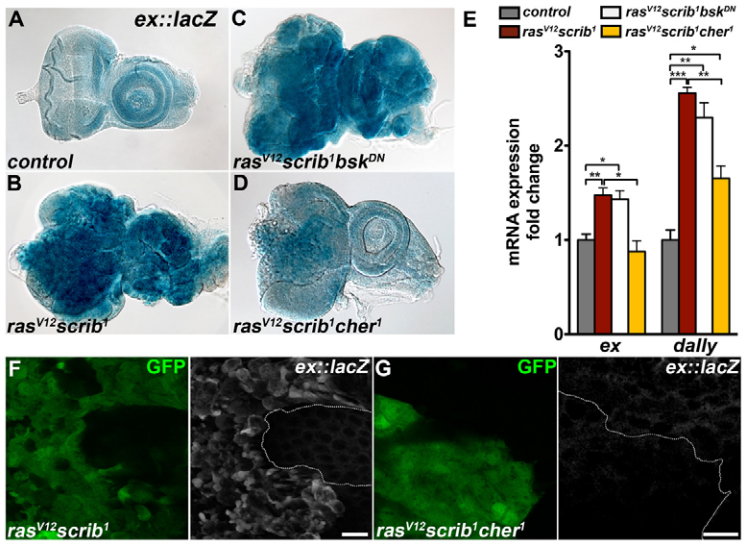

Fig. 7. Expression of Yki targets requires Cher. (**A–D**) The *ex::lacZ* reporter of Yki activity is upregulated in *ras*^{V12}*scrib*^{1} and *ras*^{V12}*scrib*^{1}*bsk*^{DN} EAD compared with control and EAD bearing *ras*^{V12}*scrib*^{1}*cher*^{1} clones. All samples were stained for the same period of time. (**E**) mRNA levels of *ex* and *dally* are significantly upregulated in *ras*^{V12}*scrib*^{1} and *ras*^{V12}*scrib*^{1}*bsk*^{DN} but not in *ras*^{V12}*scrib*^{1}*cher*^{1} mosaic EAD 6 days AEL. Data are means ± s.e.m.; $n \geq 3$; *$P<0.05$, **$P<0.01$ and ***$P<0.001$. (**F**,**G**) Immunostaining of EAD with an anti-β-Gal antibody shows that upregulation of *ex::lacZ* within the GFP-positive *ras*^{V12}*scrib*^{1} clones requires Cher. Scale bars: 10 μm.

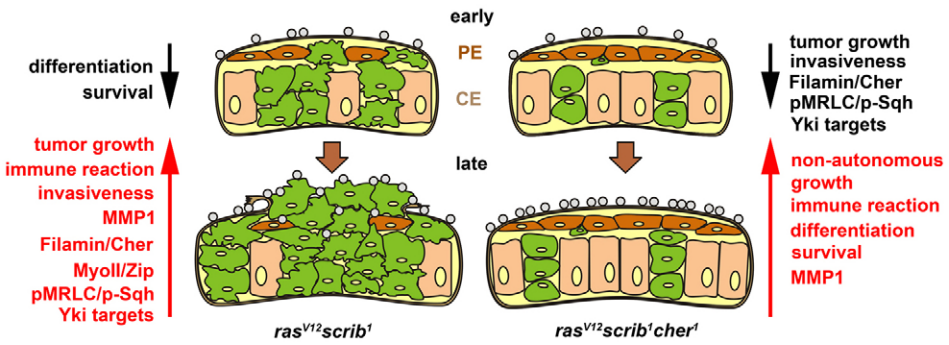

Fig. 8. Role of Filamin/Cher in tumor progression. The cartoon compares Cher-positive and Cher-deficient clonal tumors. Rapidly growing $ras^{V12}scrib^{1}$ cells (green) within peripodial epithelium (PE, dark brown) increase actomyosin contractility dependent on interaction of Cher with actin and MyoII/Zip and enrichment of phospho-myosin II regulatory light chain (pMRLC/p-Sqh). Deregulated tension stimulates Yki activity. Pressure of the tumor mass and elevated MMP1 contribute to basal membrane destruction, which in turn permits spreading of the tumor cells into neighboring tissues. Loss of Cher impedes proliferation of the tumor cells, particularly within the PE, and favors neuronal differentiation. With few tumor cells producing MMP1, the PE remains largely intact. Thus, in addition to the basal membrane, the PE provides another mechanical barrier that hinders tumor invasion. Hemocytes (gray beads) that accumulate on affected epithelia probably contribute to tumor development regardless of Cher absence CE: columnar epithelium.

multilayered masses, its expression expanded also basally. In this regard Cher expression pattern highly correlated with that of MMP1 (Uhlirova and Bohmann, 2006; supplementary material Fig. S6B,C).

Our genetic analysis clearly demonstrated the cell-autonomous requirement of Cher in the $ras^{V12}scrib^{1}$ tumors as clonal-specific *cher* removal suppressed aggressive tumor growth by reducing tumor cell proliferation, and it also suppressed tumor invasiveness while improving cell differentiation. Interestingly, in accordance with the pattern of Cher protein expression, $ras^{V12}scrib^{1}$ tumors originating in the PE seemed to be much more sensitive to Cher deficiency than those in the CE. We based this conclusion on the fact that we consistently found only few rather small clones within the PE of EAD carrying $ras^{V12}scrib^{1}cher^{1}$ tumors while numerous smaller clones were enclosed between the two epithelial layers. Our observation of filopodia-like protrusions emanating from the non-clonal cells over the $ras^{V12}scrib^{1}cher^{1}$ cells suggests that even clones originated in the PE may be forced out from the PE basally towards the CE. Sizable clones were only found at the base of the CE. Although these $ras^{V12}scrib^{1}cher^{1}$ clones grew in time, their proliferation rate was slower relative to aggressive $ras^{V12}scrib^{1}$ clones, thus permitting some animals to complete development. Even when the $ras^{V12}scrib^{1}cher^{1}$ clones reached a size of $ras^{V12}scrib^{1}$ tumors (in larvae that failed to pupate), their invasive potential was reduced.

Marked restoration of neuronal differentiation in EAD carrying $ras^{V12}scrib^{1}cher^{1}$ clones suggests a non-autonomous effect for Cher on cells within the CE. Several studies postulated a functional involvement of PE cells in disc patterning apart from their function in providing mechanical support during disc eversion (Cho et al., 2000; Gibson and Schubiger, 2000; Pallavi and Shashidhara, 2003). We speculate that disturbed integrity of PE epithelia in EAD containing $ras^{V12}scrib^{1}$ tumors might interfere with transmission of inductive signals from PE to the disc proper, thus preventing photoreceptor differentiation. The largely intact PE in EAD bearing $ras^{V12}scrib^{1}cher^{1}$ clones may still provide sufficient signal required for proper patterning. Finally, however, we cannot exclude an alternative that Cher participates in dedifferentiation of $ras^{V12}scrib^{1}$ cells.

Deficiency of Cher alters the shape of tumor cells. Although $ras^{V12}scrib^{1}cher^{1}$ cells enriched F-actin to an extent similar to invasive $ras^{V12}scrib^{1}$ cells, their shape was markedly different. Regardless of their position within the EAD, most of the $ras^{V12}scrib^{1}cher^{1}$ clonal tumors assumed round morphology, contrasting with the elongated $ras^{V12}scrib^{1}$ cells, and separated themselves from the surrounding wild-type tissue, in some cases resulting in their extrusion from the host epithelia. Work in mammalian tissue cultures and genetic studies in *Drosophila* provided evidence that even modest differences in adhesive properties guide cell sorting and segregation (Dahmann et al., 2011; Steinberg and Takeichi, 1994; Wei et al., 2005). Interestingly, endothelial cells isolated from $Flna^{-/-}$ mice showed unaltered F-actin levels and motility but displayed abnormal adherens junctions and reduced levels of VE-cadherin (Feng et al., 2006). Thus, it is plausible that cell shape changes and clonal extrusion from epithelial sheets occurring in the absence of Cher result from altered adhesive properties.

However, more recent hypotheses and experiments implicate differential mechanical tension along the cell borders as the driving force of cell sorting (Landsberg et al., 2009; Monier et al., 2010). Cellular tension is generated locally by myosin motors pulling against the actin filaments, and can act over a distance due to assembly of actin filaments into three-dimensional networks, mediated by cross-linkers such as Filamins (Gorlin et al., 1990). It has been shown that FLNA can potentiate actomyosin ATPase activity *in vitro* (Sosiński et al., 1984) and that it binds regulators of myosin-mediated contractility such as the small Rho GTPases (Rho, Rac, Cdc42) or the ROCK kinase (Nakamura et al., 2011). We have shown here that Cher binds Zip, the *Drosophila* ortholog of the nonmuscle myosin II heavy chain, and that the Cher-Zip complex is enriched in $ras^{V12}scrib^{1}$ clonal tumors. Simultaneous upregulation of p-Sqh indicates enhanced myosin ATPase and motor activity, and hence increased actomyosin contractility of tumor cells. Through its cross-linking action on the actomyosin cytoskeleton, Cher might therefore enable the tumors to maintain cell shape, proliferate and migrate even in an environment of increased mechanical stress, generated by the expanding tumor mass within the host epithelium. Thus, as a non-exclusive alternative to distorted

cell adhesion discussed above, we propose that Cher deficiency might compromise tumor cell shape stability, proliferation and spreading by reducing cell surface tension. In this regard, it is noteworthy that human melanoma cells lacking FLNA are deformed and display blebbing (Cunningham, 1995; Cunningham et al., 1992).

We have identified *cher* as a target of JNK signaling, which is required for overgrowth and invasiveness of $ras^{V12}scrib^{1}$ clonal cells. It was therefore not surprising that loss of Cher affected invasive $ras^{V12}scrib^{1}$ tumors in a way similar to inhibited JNK activity, namely by limiting tumor growth, suppressing tumor invasiveness, and restoring cell differentiation (Igaki et al., 2006; Leong et al., 2009; Uhlirova and Bohmann, 2006). However, the impact of removed *cher* function on reduced malignity of $ras^{V12}scrib^{1}$ tumors exceeded the effect of compromised JNK activity. This was reflected by survival to adulthood of animals bearing $ras^{V12}scrib^{1}cher^{1}$ clones but not $ras^{V12}scrib^{1}bsk^{DN}$ clones. One explanation for the stronger effect of *cher* mutation is that whereas a basal uninduced level of Cher expression persisted in the presence of the dominant-negative form of Bsk, the $cher^{1}$ allele caused a complete loss of function. Alternatively, Cher could promote the growth of $ras^{V12}scrib^{1}$ tumors through other mechanisms.

The loss of *scrib* has been recently shown to contribute to the overgrowth of the $ras^{V12}scrib^{1}$ clonal tissue independently of JNK, by inhibiting the tumor-suppressor Hpo pathway (Doggett et al., 2011). A link between actin cytoskeleton dynamics and Hpo signaling has been supported by studies in *Drosophila* and mammalian cell culture systems (Fernández et al., 2011; Sansores-Garcia et al., 2011; Wada et al., 2011; Zhao et al., 2012). Furthermore, manipulating filamentous actin in developing imaginal discs results in Yki-dependent tissue overgrowth (Fernández et al., 2011; Sansores-Garcia et al., 2011). Here we have demonstrated that the actin cross-linker Cher promotes tumor growth, and based on Cher-dependent deregulation of two Yki targets, *expanded* and *dally*, we speculate that Cher does so at least in part by modulating the Hpo/Yki pathway. Clearly, the exact mechanism how Filamin/Cher interacts with this pathway awaits elucidation. It is conceivable that some components of Hpo/Yki signaling sense mechanical cues effected by Cher on the actomyosin network. Our results hint that it might be the tension generated by myosin motor activity driving tumor proliferation of $ras^{V12}scrib^{1}$ tumors. This would agree with a recent discovery that activity of mammalian Yki homologues YAP and TAZ requires stress fibers and Rho (Dupont et al., 2011). Research in this direction can elucidate how growth-promoting signaling pathways hijack the cytoskeletal network during tumorigenesis.

Materials and Methods

Plasmids and antibody production

AP-1 binding sites in the *Drosophila cher* gene were predicted using the Transcription Element Search System (TESS) (Schug, 2008) (http://www.cbil.upenn.edu/cgi-bin/tess). For construction of $cher^{wt}$*::RFP*, TPA DNA response elements in *TRE::RFP* vector (Chatterjee and Bohmann, 2012) were replaced with a 1.4-kb sequence upstream of the first *cher* exon, amplified using *SphI-cher-prom for* and *XhoI-cher-prom rev* primers (supplementary material Table S1). $cher^{mut}$*::RFP* was prepared by mutating all four AP-1 binding sites within the $cher^{wt}$*::RFP* plasmid using the QuikChange Lightning Multi Site-Directed Mutagenesis Kit (Agilent Technologies) with primers *cher-prom-ap1-A, B, C* and *D for* (supplementary material Table S1). To raise anti-Cher antibody, a *Drosophila cher* cDNA fragment encoding amino acids 189–482 was cloned into the pET28b plasmid. Rats were immunized (Eurogentec) with bacterially expressed protein, which was purified using the hexahistidine tag.

Fly strains and clonal analysis

Generation of mosaics in eye/antennal imaginal discs using the Mosaic analysis with a repressible cell marker method (MARCM) (Lee and Luo, 2001) was carried out as described (Uhlirova et al., 2005) using the following mutant and transgenic fly strains: (1) *ey-FLP1; Act* $>y^{+}>$*Gal4, UAS-GFP; FRT82B, Tub-Gal80*, (2) *w;; FRT82B*, (3) *w; UAS-*ras^{V12}*; FRT82B* $scrib^{1}$*/TM6B*, (4) *w; UAS-*ras^{V12}*; FRT82B* $scrib^{1}$ *UAS-*bsk^{DN}*/TM6B*, (5) *w; UAS-*ras^{V12}*; FRT82B* $scrib^{1}kay^{3}$ (6) *w; UAS-*$cher^{IR}$ (VDRC, Tr. ID-107451), (7) *w; UAS-*$cher^{IR}$*; FRT82B/TM6B*, (8) *w; UAS-*ras^{V12} *UAS-*$cher^{IR}$*/CyO; FRT82B scrib1/TM6B att.*, (9) *w;; FRT82B* $cher^{1}$*/TM6B*, (10) *w; UAS-*ras^{V12}*; FRT82B* $scrib^{1}$ $cher^{1}$*/TM6B*, (11) *w; UAS-*hep^{act}, *UAS-*ras^{V12}*; FRT82B*, (12) *w; UAS-*zip^{IR} (VDRC, Tr. ID-7819), (13) *w; UAS-*ras^{V12}, *UAS-*zip^{IR}; *FRT82B* $scrib^{1}$, (14) ex^{697} (*ex::lacZ*). All crosses were carried out at 25°C. $cher^{1}$ (Robinson et al., 1997) and kay^{3} mutant lines were a gift from Lynn Cooley (New Haven, CT) and Constantin Yanicostas (Institut Jacques Monod, Paris, France), respectively. For TARGET inducible expression, *T80-Gal4, UAS-EGFP/CyO; tub-Gal80*^{ts}*/TM6B att.* females were crossed to control (w^{1118}) and *w; UAS-*Hep^{wt} males, respectively. Progeny was kept at 18°C until early third-instar. Larvae were heat-shocked at 37°C for 60 min. Total RNA was isolated after additional 6 h of incubation at 29°C.

Quantification of tumor invasiveness and pupation rate

More than 100 third-instar larval brains (7 days AEL) from each genotype were dissected, fixed and mounted. The degree of malignancy was determined by analyzing blind samples under a fluorescent microscope. The genotypes were disclosed to the observer only after the count to ensure unbiased results. Arbitrary degrees of invasive tumors were: (0) noninvasive, (1) clonal cells overgrow one of the optic lobes and invade the VNC, (2) both optic lobes are overgrown by mutant tissue and cells enter the VNC from both sides, and (3) optic lobes and most of the VNC are invaded by clonal tissue. Statistical significance was determined using a chi-square test (Prism). Pupae were counted on days 8 and 9 AEL. Percentage was calculated from 100 animals per experiment with at least three replicates. Statistical significance was determined using one-way ANOVA followed by the Unequal H HSD test.

Tissue staining

Dissected imaginal discs and brains were fixed in 4% paraformaldehyde in PBST (PBS and 0.1% Triton X-100) for 25 min, washed and blocked in PBST containing 0.5% BSA. The following primary antibodies were used for overnight staining at 4°C: rat anti-Cher (1:1000), rat anti-N-Fil (1:1000) (Sokol and Cooley, 1999), mouse anti-MMP1 (1:300, DSHB 14A3D2), mouse anti-H2 (1:500) (Kurucz et al., 2003), chicken anti-Zipper (1:500, a gift from Eric Wieschaus), rabbit anti-pH 3 (1:100, Cell Signaling Technology), rabbit anti-activated caspase 3 (1:500, Cell Signaling Technology), rabbit anti-phospho MRLC (Ser19) (1:100, Cell Signaling Technology), and rat anti-Elav (1:200; 7E8A10) and mouse anti-Fasciclin III (1:300, 7G10), both from Developmental Studies Hybridoma Bank (Iowa). After washing, samples were incubated with a corresponding secondary antibody coupled to Rhodamine (TRITC), Cy3 or Cy5 (Jackson ImmunoResearch) for 2 h. Samples were counterstained with Alexa 456-phalloidin (Invitrogen) and DAPI or Hoechst (Invitrogen) to visualize actin filaments and nuclei, respectively. The *ex::lacZ* activity was detected in mosaic EAD using a standard X-Gal (5-bromo-4-chloro-3-indolyl-β-D-galactopyranoside) staining procedure.

Image acquisition and processing

Confocal stacks were acquired at room temperature with Olympus FV1000 confocal microscope equipped with 20× UPlan S-Apo (NA 0.85), 40× UPlan FL (NA 1.30) and 60× UPlanApo (NA 1.35) objectives. Maximum projections were generated using Fluoview 2.1c Software (Olympus) and Image J (Abramoff et al., 2004), and transversal sections using Imaris 7.0.0 (Bitplane). Final image processing including panel assembly, brightness and contrast adjustment were done in Photoshop CS4 (Adobe Systems, Inc.). Z-stacks of adult eyes were taken using motorized Leica M165 FC fluorescent stereomicroscope equipped with DFC490 CCD camera and GFP2 (Ex. 480/40 nm) filter set. Images were processed using the Multifocus module of LAS 3.7.0 software (Leica).

Drosophila S2 cell culture, transfection and immunostaining

S2 Schneider cells were cultured at 25°C in Shields and Sang M3 insect medium (Sigma-Aldrich) containing 8% fetal bovine serum and antibiotics (Pen/Strep; Gibco). Prior to transfection, cells were starved in serum-free medium for 30 min and subsequently transfected using Fugene HD (Roche Applied Science) according to manufacturer's instructions. Immunostaining was performed as described (Jindra et al., 2004).

Semi-quantitative and quantitative RT-PCR

Total RNA was isolated from EADs dissected from third-instar larvae (6 or 7 days AEL) using TRIzol (Invitrogen), and 2 μg of DNase-treated RNA were transcribed using Superscript III reverse transcriptase with oligo (dT) primers (Invitrogen). Semi-quantitative PCR was carried out using ExTaq Polymerase (Takara Bio Inc.) in 26 standard temperature cycles. Quantitative RT-PCR was performed with

Power SyBR Green PCR master mix (Applied Biosystems) using the 7900HT Fast Real-Time PCR System (Applied Biosystems). All qPCR primers (supplementary material Table S1) were designed to anneal at 62℃. All data were normalized to *rp49* transcript levels, and fold changes in gene expression were calculated using the Relative standard curve method (Larionov et al., 2005). At least 4–6 biological replicates were analyzed per experiment. Statistical significance was determined using the unpaired two-tailed Student's *t*-test with unequal variance.

Flow cytometry (FACS)

Dissected EAD were dissociated into cell suspension by incubating in 10×Trypsin/EDTA/PBS for 45 min and by subsequent passing through insulin syringe with a 0.33-mm diameter needle (Terumo). Cell counting based on GFP fluorescence was performed using a FACSCalibur Flow Cytometer (BD Biosciences). For analysis of mitosis and apoptosis EAD cells were fixed and permeabilized using the IntraSure kit (BD Biosciences). Upon staining with the following antibodies: rabbit anti-cleaved caspase-3 (PE Conjugate), rabbit anti-pH 3 (Alexa-647 Conjugate, both from Cell Signaling Technology) and anti-GFP (AL-488-conjugated, Invitrogen), for 30 min at RT, cells were incubated in BD Stabilizing Fixative (BD Biosciences) and analyzed on a FACS Aria III flow cytometer (BD Biosciences). Data (>10,000 events/sample, four biological replicates) were analyzed using FACS Diva software (BD Biosciences).

Immunoprecipitation

Dissected EAD (80 per genotype) were lysed in 50 mM TRIS (pH 7.8), 150 mM NaCl, 1 mM EDTA (pH 8.0), 1% Triton-X100, 0.01% Igepal, protease inhibitors (Roche). After 10 minutes of incubation on ice, lysates were centrifuged at 12,000 ***g*** for 10 min at 4℃. Protein concentration of supernatant was determined using the BioRad protein assay, and supernatant (500 µg of total protein) was incubated overnight with a rat anti-Cheerio antibody (1:200) at 4℃. The antibody complexes were captured using 30 µl of equilibrated Dynabeads Protein G (Invitrogen) for 4 h at 4℃. After five washes in lysis buffer, proteins were recovered in two consecutive elution steps, each with 50 µl of 0.1 M glycine-HCl (pH 3.0) for 5 min. After neutralization with 10 µl of 0.5 M Tris-HCl (pH 7.8) and 1.5 M NaCl, proteins were subjected to SDS-PAGE and detected by immunoblotting with the appropriate antibodies, followed by enhanced chemiluminescence using ImageQuant LAS4000 reader (GE Healthcare).

Acknowledgements

We are grateful to Lynn Cooley, Dirk Bohmann, Eric Wieschaus, Constantin Yanicostas, István Andó, the Bloomington Center (Bloomington, USA), the VDRC (Vienna, Austria) and the DSHB (Iowa, USA) for fly stocks, plasmids and antibodies. We thank Christoph Göttlinger, Gunter Rappl and Hinrich Abken for help with FACS analysis, Tobias Lamkemeyer for help with protein purification, Peter Frommolt for help with qRT-PCR analyses, Astrid Schauss for advice with image quantifications, Sabrina Jung for technical help, and Marek Jindra for discussion and critical reading of the manuscript. The authors declare no conflict of interest.

Author contributions

E.K. and M.U. conceived, designed and performed the experiments, analyzed the data, interpreted the results and wrote the manuscript.

Funding

This work was supported by the following grants to M.U.: Sofja Kovalevskaja Award from the Alexander von Humboldt Foundation (AvH, Germany), CECAD funds and CRC 832, both from the German Research Council (DFG, Germany).

Supplementary material available online at
http://jcs.biologists.org/lookup/suppl/doi:10.1242/jcs.114462/-/DC1

References

Abramoff, M., Magalhaes, P. and Ram, S. (2004). Image processing with ImageJ. *Biophotonics International* **11**, 36-42. http://igitur-archive.library.uu.nl/med/2011-0512-200507/UUindex.html

Ai, J., Huang, H., Lv, X., Tang, Z., Chen, M., Chen, T., Duan, W., Sun, H., Li, Q., Tan, R. et al. (2011). FLNA and PGK1 are two potential markers for progression in hepatocellular carcinoma. *Cell. Physiol. Biochem.* **27**, 207-216.

Alper, Ö., Stetler-Stevenson, W. G., Harris, L. N., Leitner, W. W., Özdemirli, M., Hartmann, D., Raffeld, M., Abu-Asab, M., Byers, S., Zhuang, Z. et al. (2009). Novel anti-filamin-A antibody detects a secreted variant of filamin-A in plasma from patients with breast carcinoma and high-grade astrocytoma. *Cancer Sci.* **100**, 1748-1756.

Baena-Lopez, L. A., Rodríguez, I. and Baonza, A. (2008). The tumor suppressor genes *dachsous* and *fat* modulate different signalling pathways by regulating *dally* and *dally-like*. *Proc. Natl. Acad. Sci. USA* **105**, 9645-9650.

Bedolla, R. G., Wang, Y., Asuncion, A., Chamie, K., Siddiqui, S., Mudryj, M. M., Prihoda, T. J., Siddiqui, J., Chinnaiyan, A. M., Mehra, R. et al. (2009). Nuclear versus cytoplasmic localization of filamin A in prostate cancer: immunohistochemical correlation with metastases. *Clin. Cancer Res.* **15**, 788-796.

Boedigheimer, M. and Laughon, A. (1993). Expanded: a gene involved in the control of cell proliferation in imaginal discs. *Development* **118**, 1291-1301.

Brumby, A. M. and Richardson, H. E. (2003). *scribble* mutants cooperate with oncogenic Ras or Notch to cause neoplastic overgrowth in *Drosophila*. *EMBO J.* **22**, 5769-5779.

Brumby, A. M., Goulding, K. R., Schlosser, T., Loi, S., Galea, R., Khoo, P., Bolden, J. E., Aigaki, T., Humbert, P. O. and Richardson, H. E. (2011). Identification of novel Ras-cooperating oncogenes in *Drosophila melanogaster*: a RhoGEF/Rho-family/JNK pathway is a central driver of tumorigenesis. *Genetics* **188**, 105-125.

Butcher, D. T., Alliston, T. and Weaver, V. M. (2009). A tense situation: forcing tumour progression. *Nat. Rev. Cancer* **9**, 108-122.

Castoria, G., D'Amato, L., Ciociola, A., Giovannelli, P., Giraldi, T., Sepe, L., Paolella, G., Barone, M. V., Migliaccio, A. and Auricchio, F. (2011). Androgen-induced cell migration: role of androgen receptor/filamin A association. *PLoS ONE* **6**, e17218.

Chatterjee, N. and Bohmann, D. (2012). A versatile ΦC31 based reporter system for measuring AP-1 and Nrf2 signaling in *Drosophila* and in tissue culture. *PLoS ONE* **7**, e34063.

Cho, K. O., Chern, J., Izaddoost, S. and Choi, K. W. (2000). Novel signaling from the peripodial membrane is essential for eye disc patterning in *Drosophila*. *Cell* **103**, 331-342.

Cordero, J. B., Macagno, J. P., Stefanatos, R. K., Strathdee, K. E., Cagan, R. L. and Vidal, M. (2010). Oncogenic Ras diverts a host TNF tumor suppressor activity into tumor promoter. *Dev. Cell* **18**, 999-1011.

Coso, O. A., Chiariello, M., Yu, J. C., Teramoto, H., Crespo, P., Xu, N., Miki, T. and Gutkind, J. S. (1995). The small GTP-binding proteins Rac1 and Cdc42 regulate the activity of the JNK/SAPK signaling pathway. *Cell* **81**, 1137-1146.

Cunningham, C. C. (1995). Actin polymerization and intracellular solvent flow in cell surface blebbing. *J. Cell Biol.* **129**, 1589-1599.

Cunningham, C. C., Gorlin, J. B., Kwiatkowski, D. J., Hartwig, J. H., Janmey, P. A., Byers, H. R. and Stossel, T. P. (1992). Actin-binding protein requirement for cortical stability and efficient locomotion. *Science* **255**, 325-327.

Dahmann, C., Oates, A. C. and Brand, M. (2011). Boundary formation and maintenance in tissue development. *Nat. Rev. Genet.* **12**, 43-55.

Doggett, K., Grusche, F. A., Richardson, H. E. and Brumby, A. M. (2011). Loss of the *Drosophila* cell polarity regulator Scribbled promotes epithelial tissue overgrowth and cooperation with oncogenic Ras-Raf through impaired Hippo pathway signaling. *BMC Dev. Biol.* **11**, 57.

Dupont, S., Morsut, L., Aragona, M., Enzo, E., Giulitti, S., Cordenonsi, M., Zanconato, F., Le Digabel, J., Forcato, M., Bicciato, S. et al. (2011). Role of YAP/TAZ in mechanotransduction. *Nature* **474**, 179-183.

Feng, Y., Chen, M. H., Moskowitz, I. P., Mendonza, A. M., Vidali, L., Nakamura, F., Kwiatkowski, D. J. and Walsh, C. A. (2006). Filamin A (FLNA) is required for cell-cell contact in vascular development and cardiac morphogenesis. *Proc. Natl. Acad. Sci. USA* **103**, 19836-19841.

Fernández, B. G., Gaspar, P., Brás-Pereira, C., Jezowska, B., Rebelo, S. R. and Janody, F. (2011). Actin-Capping Protein and the Hippo pathway regulate F-actin and tissue growth in *Drosophila*. *Development* **138**, 2337-2346.

Field, C. M. and Alberts, B. M. (1995). Anillin, a contractile ring protein that cycles from the nucleus to the cell cortex. *J. Cell Biol.* **131**, 165-178.

Friedl, P. and Alexander, S. (2011). Cancer invasion and the microenvironment: plasticity and reciprocity. *Cell* **147**, 992-1009.

Gibson, M. C. and Schubiger, G. (2000). Peripodial cells regulate proliferation and patterning of *Drosophila* imaginal discs. *Cell* **103**, 343-350.

Gorlin, J. B., Yamin, R., Egan, S., Stewart, M., Stossel, T. P., Kwiatkowski, D. J. and Hartwig, J. H. (1990). Human endothelial actin-binding protein (ABP-280, nonmuscle filamin): a molecular leaf spring. *J. Cell Biol.* **111**, 1089-1105.

Hamaratoglu, F., Willecke, M., Kango-Singh, M., Nolo, R., Hyun, E., Tao, C., Jafar-Nejad, H. and Halder, G. (2006). The tumour-suppressor genes NF2/Merlin and Expanded act through Hippo signalling to regulate cell proliferation and apoptosis. *Nat. Cell Biol.* **8**, 27-36.

Hanahan, D. and Weinberg, R. A. (2011). Hallmarks of cancer: the next generation. *Cell* **144**, 646-674.

Holz, A., Bossinger, B., Strasser, T., Janning, W. and Klapper, R. (2003). The two origins of hemocytes in *Drosophila*. *Development* **130**, 4955-4962.

Igaki, T., Pagliarini, R. A. and Xu, T. (2006). Loss of cell polarity drives tumor growth and invasion through JNK activation in *Drosophila*. *Curr. Biol.* **16**, 1139-1146.

Jindra, M., Gaziova, I., Uhlirova, M., Okabe, M., Hiromi, Y. and Hirose, S. (2004). Coactivator MBF1 preserves the redox-dependent AP-1 activity during oxidative stress in *Drosophila*. *EMBO J.* **23**, 3538-3547.

Karess, R. E., Chang, X.-J., Edwards, K. A., Kulkarni, S., Aguilera, I. and Kiehart, D. P. (1991). The regulatory light chain of nonmuscle myosin is encoded by *spaghetti-squash*, a gene required for cytokinesis in *Drosophila*. *Cell* **65**, 1177-1189.

Kockel, L., Homsy, J. G. and Bohmann, D. (2001). *Drosophila* AP-1: lessons from an invertebrate. *Oncogene* **20**, 2347-2364.
Kurucz, E., Zettervall, C.-J., Sinka, R., Vilmos, P., Pivarcsi, A., Ekengren, S., Hegedüs, Z., Andó, I. and Hultmark, D. (2003). Hemese, a hemocyte-specific transmembrane protein, affects the cellular immune response in *Drosophila*. *Proc. Natl. Acad. Sci. USA* **100**, 2622-2627.
Landsberg, K. P., Farhadifar, R., Ranft, J., Umetsu, D., Widmann, T. J., Bittig, T., Said, A., Jülicher, F. and Dahmann, C. (2009). Increased cell bond tension governs cell sorting at the *Drosophila* anteroposterior compartment boundary. *Curr. Biol.* **19**, 1950-1955.
Larionov, A., Krause, A. and Miller, W. (2005). A standard curve based method for relative real time PCR data processing. *BMC Bioinformatics* **6**, 62.
Lee, T. and Luo, L. (2001). Mosaic analysis with a repressible cell marker (MARCM) for *Drosophila* neural development. *Trends Neurosci.* **24**, 251-254.
Leong, G. R., Goulding, K. R., Amin, N., Richardson, H. E. and Brumby, A. M. (2009). Scribble mutants promote aPKC and JNK-dependent epithelial neoplasia independently of Crumbs. *BMC Biol.* **7**, 62.
Li, M. G., Serr, M., Edwards, K., Ludmann, S., Yamamoto, D., Tilney, L. G., Field, C. M. and Hays, T. S. (1999). Filamin is required for ring canal assembly and actin organization during *Drosophila* oogenesis. *J. Cell Biol.* **146**, 1061-1074.
Liu, R., Linardopoulou, E. V., Osborn, G. E. and Parkhurst, S. M. (2010). Formins in development: orchestrating body plan origami. *Biochim. Biophys. Acta* **1803**, 207-225.
Marinissen, M. J., Chiariello, M., Tanos, T., Bernard, O., Narumiya, S. and Gutkind, J. S. (2004). The small GTP-binding protein RhoA regulates c-jun by a ROCK-JNK signaling axis. *Mol. Cell* **14**, 29-41.
Martín-Blanco, E., Gampel, A., Ring, J., Virdee, K., Kirov, N., Tolkovsky, A. M. and Martinez-Arias, A. (1998). *puckered* encodes a phosphatase that mediates a feedback loop regulating JNK activity during dorsal closure in *Drosophila*. *Genes Dev.* **12**, 557-570.
McGuire, S. E., Le, P. T., Osborn, A. J., Matsumoto, K. and Davis, R. L. (2003). Spatiotemporal rescue of memory dysfunction in Drosophila. *Science* **302**, 1765-1768.
Minden, A., Lin, A., Claret, F. X., Abo, A. and Karin, M. (1995). Selective activation of the JNK signaling cascade and c-Jun transcriptional activity by the small GTPases Rac and Cdc42Hs. *Cell* **81**, 1147-1157.
Monier, B., Pélissier-Monier, A., Brand, A. H. and Sanson, B. (2010). An actomyosin-based barrier inhibits cell mixing at compartmental boundaries in *Drosophila* embryos. *Nat. Cell Biol.* **12**, 60-65, 1-9.
Nakamura, F., Stossel, T. P. and Hartwig, J. H. (2011). The filamins: organizers of cell structure and function. *Cell Adh. Migr.* **5**, 160-169.
Nallapalli, R. K., Ibrahim, M. X., Zhou, A. X., Bandaru, S., Sunkara, S. N., Redfors, B., Pazooki, D., Zhang, Y., Borén, J., Cao, Y. et al. (2012). Targeting filamin A reduces K-RAS-induced lung adenocarcinomas and endothelial response to tumor growth in mice. *Mol. Cancer* **11**, 50.
Nürnberg, A., Kitzing, T. and Grosse, R. (2011). Nucleating actin for invasion. *Nat. Rev. Cancer* **11**, 177-187.
Pagliarini, R. A. and Xu, T. (2003). A genetic screen in *Drosophila* for metastatic behavior. *Science* **302**, 1227-1231.
Pallavi, S. K. and Shashidhara, L. S. (2003). Egfr/Ras pathway mediates interactions between peripodial and disc proper cells in *Drosophila* wing discs. *Development* **130**, 4931-4941.
Pallavi, S. K. and Shashidhara, L. S. (2005). Signaling interactions between squamous and columnar epithelia of the *Drosophila* wing disc. *J. Cell Sci.* **118**, 3363-3370.
Pastor-Pareja, J. C., Wu, M. and Xu, T. (2008). An innate immune response of blood cells to tumors and tissue damage in *Drosophila*. *Dis. Model. Mech.* **1**, 144-154, discussion 153.
Pollard, T. D. and Cooper, J. A. (2009). Actin, a central player in cell shape and movement. *Science* **326**, 1208-1212.
Popowicz, G. M., Schleicher, M., Noegel, A. A. and Holak, T. A. (2006). Filamins: promiscuous organizers of the cytoskeleton. *Trends Biochem. Sci.* **31**, 411-419.
Richardson, H. E. (2011). Actin up for Hippo. *EMBO J.* **30**, 2307-2309.
Robinson, D. N., Smith-Leiker, T. A., Sokol, N. S., Hudson, A. M. and Cooley, L. (1997). Formation of the *Drosophila* ovarian ring canal inner rim depends on cheerio. *Genetics* **145**, 1063-1072.
Sansores-Garcia, L., Bossuyt, W., Wada, K.-I., Yonemura, S., Tao, C., Sasaki, H. and Halder, G. (2011). Modulating F-actin organization induces organ growth by affecting the Hippo pathway. *EMBO J.* **30**, 2325-2335.
Schug, J. (2008). *Current Protocols in Bioinformatics* (ed. A. D. Baxevanis, G. A. Petsko, L. D. Stein and G. D. Stormo). Hoboken, NJ: Current Protocols in Bioinformatics.
Sokol, N. S. and Cooley, L. (1999). *Drosophila* filamin encoded by the *cheerio* locus is a component of ovarian ring canals. *Curr. Biol.* **9**, 1221–1230.
Sosiński, J., Szpacenko, A. and Dabrowska, R. (1984). Potentiation of actomyosin ATPase activity by filamin. *FEBS Lett.* **178**, 311-314.
Srivastava, A., Pastor-Pareja, J. C., Igaki, T., Pagliarini, R. and Xu, T. (2007). Basement membrane remodeling is essential for *Drosophila* disc eversion and tumor invasion. *Proc. Natl. Acad. Sci. USA* **104**, 2721-2726.
Steinberg, M. S. and Takeichi, M. (1994). Experimental specification of cell sorting, tissue spreading, and specific spatial patterning by quantitative differences in cadherin expression. *Proc. Natl. Acad. Sci. USA* **91**, 206-209.
Uhlirova, M. and Bohmann, D. (2006). JNK- and Fos-regulated Mmp1 expression cooperates with Ras to induce invasive tumors in *Drosophila*. *EMBO J.* **25**, 5294-5304.
Uhlirova, M., Jasper, H. and Bohmann, D. (2005). Non-cell-autonomous induction of tissue overgrowth by JNK/Ras cooperation in a *Drosophila* tumor model. *Proc. Natl. Acad. Sci. USA* **102**, 13123-13128.
Wada, K.-I., Itoga, K., Okano, T., Yonemura, S. and Sasaki, H. (2011). Hippo pathway regulation by cell morphology and stress fibers. *Development* **138**, 3907-3914.
Wagner, E. F. and Nebreda, A. R. (2009). Signal integration by JNK and p38 MAPK pathways in cancer development. *Nat. Rev. Cancer* **9**, 537-549.
Wei, S.-Y., Escudero, L. M., Yu, F., Chang, L.-H., Chen, L.-Y., Ho, Y.-H., Lin, C.-M., Chou, C.-S., Chia, W., Modolell, J. et al. (2005). Echinoid is a component of adherens junctions that cooperates with DE-Cadherin to mediate cell adhesion. *Dev. Cell* **8**, 493-504.
Xia, Y. and Karin, M. (2004). The control of cell motility and epithelial morphogenesis by Jun kinases. *Trends Cell Biol.* **14**, 94-101.
Xu, Y., Bismar, T. A., Su, J., Xu, B., Kristiansen, G., Varga, Z., Teng, L., Ingber, D. E., Mammoto, A., Kumar, R. et al. (2010). Filamin A regulates focal adhesion disassembly and suppresses breast cancer cell migration and invasion. *J. Exp. Med.* **207**, 2421-2437.
Zhao, B., Li, L., Wang, L., Wang, C. Y., Yu, J. and Guan, K. L. (2012). Cell detachment activates the Hippo pathway via cytoskeleton reorganization to induce anoikis. *Genes Dev.* **26**, 54-68.